PHYSICAL REVIEW D **80,** 075005 (2009)

Supersymmetric corrections to the threshold production of top quark pairs

Y. Kiyo, M. Steinhauser, and N. Zerf

Institut für Theoretische Teilchenphysik, Universität Karlsruhe, Karlsruhe Institute of Technology (KIT), 76128 Karlsruhe, Germany

(Received 7 July 2009; published 7 October 2009)

In this paper we investigate supersymmetric effects to the threshold production cross section of top-quark pairs in electron positron annihilation. In particular, we consider the complete one-loop corrections from the strong and weak sector of the minimal supersymmetric standard model.

DOI: 10.1103/PhysRevD.80.075005 PACS numbers: 11.30.Pb, 13.66.Bc, 14.65.Ha

I. INTRODUCTION

One of the main goals of a future electron positron collider is the precise measurement of the top-quark production cross section in the threshold region. The comparison to the theoretical prediction allows for a precise extraction of the top-quark mass, its width, the strong coupling and—in case the Higgs boson is not too heavy—the top-quark Yukawa coupling.

The next-to-next-to-leading order (NNLO) QCD corrections to the total cross section $\sigma(e^+e^- \to t\bar{t})$ has been completed several years ago [1]. One observes large perturbative corrections from the second order terms which make a precise prediction difficult. In the recent years a big effort has been undertaken to complete the third-order corrections to $\sigma(e^+e^- \to t\bar{t})$ [2–12]. First numerical estimates [13] indicate that the convergence of the perturbation theory is improved after the inclusion of the NNNLO terms. In addition to the third-order corrections also the resummation of the NNLL terms is studied [14–16].

In order to profit from precise experimental measurements it is desired to reach an uncertainty below approximately 3% from the theory side [17]. Radiative corrections of this order can easily be reached by effects from theories beyond the standard model (SM). An attractive extension of the SM is Supersymmetry and, in particular, the minimal supersymmetric standard model (MSSM) which answers several open questions of the SM. For example, it stabilizes the Higgs boson mass at the electroweak scale, provides a dark matter candidate, and allows for the unification of the couplings. For this reason we consider in this paper the MSSM where the complete one-loop corrections both in the strong and electroweak (nonphotonic) sector of the theory are considered. Furthermore we confirm the results from Refs. [18–21] obtained in the framework of the SM and two-Higgs-doublet model (THDM) of type II, respectively.

It is convenient to perform the calculation of the production cross section in the framework of an effective theory where the produced top quarks are described by a nonrelativistic two-particle Green's function. All effects connected to energy scales above $\mu \approx m_W$ are contained in coefficient functions which represent the new couplings in the effective Lagrangian. Since the masses of the supersymmetric particles are above the electroweak scale they only influence the matching coefficients of the effective operators. For the top-quark production we have to consider the vector current in the full and effective theory which constitutes a building block for all threshold phenomena involving the coupling of the initial electron and positron via photon, Z boson or box diagrams to heavy quarks.

The remainder of the paper is organized as follows: In the next section we provide the formulas which are necessary for the evaluation of the threshold cross section. Afterwards we discuss the numerical effects from the strong and weak sector of the MSSM in Secs. III and IV and present our conclusions in Sec. V.

II. FRAMEWORK

Nonrelativistic QCD (NRQCD) allows for a consistent separation of the hard corrections connected to energy scales of the order of the weak gauge bosons or higher from the soft scales which are involved in the top antitop bound state. Within NRQCD we can normalize the production cross section to $\sigma(e^+e^- \to \mu^+\mu^-) = (4\pi\alpha^2)/(3s)$ and denote the ratio by R

$$R(e_L^+e_R^- \to t\bar{t}X) = \frac{8\pi}{s}\,\mathrm{Im}[(h_{R,V})^2 H_V + (h_{R,A})^2 H_A], \quad (1)$$

where s is the square of the center-of-mass energy. In Eq. (1) left-handed positrons and right-handed electrons are considered; for $e_R^+e_L^-$ in the initial state a similar expression is obtained by replacing R by L in Eq. (1). Note that the initial states $e_R^+e_R^-$ and $e_L^+e_L^-$ are suppressed by a factor $(m_e/M_W)^2 \sim 10^{-10}$ and are thus negligible. $h_{R,V}$ and $h_{R,A}$ are so-called helicity amplitudes which absorb the matching coefficients representing the coupling of the effective operators. They take care of the hard part of the reaction. The first subscript of h refers to helicity of the electron, and the second one to the vector ($J_V^\mu = \bar{\psi}\gamma^\mu\psi$) or axial-vector coupling ($J_A^\mu = \bar{\psi}\gamma^\mu\gamma_5\psi$) of the gauge bosons to the top-quark current. In this paper we evaluate corrections to $h_{R,V}$ and $h_{L,V}$.

The bound-state dynamics is contained in the so-called hadronic part formed by current-current correlators within NRQCD. They are denoted by H_V and H_A in Eq. (1) and

will not be considered further in this paper. At threshold the contribution from the axial-vector current is suppressed by two powers of top-quark velocity thus we only consider the vector current J_V^μ in this work. Its counterpart in the effective theory reads $j_V^i = \psi^\dagger \sigma^i \chi$.

It is convenient to separate the photon and Z contribution in $h_{I,V}^{\rm tree}$ and write

$$h_{I,V}^{\rm tree} = h_{I,V}^{\gamma,\rm tree} + h_{I,V}^{Z,\rm tree}. \tag{2}$$

Here the tree-level contributions are given by ($I = L, R$)

$$\begin{aligned} h_{I,V}^{\gamma,\rm tree} &= Q_e Q_t, \qquad h_{I,V}^{Z,\rm tree} = \frac{s\beta_I^e \beta_V^t}{s - M_Z^2}, \\ \beta_V^t &= \frac{\beta_R^t + \beta_L^t}{2}, \qquad \beta_I^f = \frac{(T_3)_{f_I} - s_w^2 Q_f}{s_w c_w}, \end{aligned} \tag{3}$$

where the β_I^f is the coupling of a fermion ($f = e, t$) to the Z boson, s_w is the sine of the weak mixing angle ($c_w^2 = 1 - s_w^2 = m_W^2/m_Z^2$), and electric and isospin charges for top quark and electron are given by

$$\begin{aligned} Q_e = -1, \qquad Q_t = 2/3, \qquad (T_3)_{t_L} = 1/2, \\ (T_3)_{e_L} = -1/2, \qquad (T_3)_{f_R} \equiv 0. \end{aligned} \tag{4}$$

In the following the abbreviation $T_3^f \equiv (T_3)_{f_L}$ will be used. Let us note that $h_{I,A}$ can be obtained by substituting β_V^t by $\beta_A^t = (\beta_R^t - \beta_L^t)/2$ in formula (3). The loop corrections are taken into account via

$$h_{I,V} = h_{I,V}^{\rm tree} + h_{I,V}^X, \tag{5}$$

where X stands for QCD, SQCD (supersymmetric QCD), SM, THDM,[1] or MSSM. The numerical effects are discussed for the quantity

$$\Delta^X = \frac{\delta R^X}{R^{\rm LO}} = \frac{2h_{L,V}^{\rm tree}\,{\rm Re}(h_{L,V}^X) + 2h_{R,V}^{\rm tree}\,{\rm Re}(h_{R,V}^X)}{(h_{L,V}^{\rm tree})^2 + (h_{R,V}^{\rm tree})^2}, \tag{6}$$

where the sum over all helicity states of the incoming electron and positron has been performed. Let us note that in our case for the evaluation of $h_{I,V}$ one has to set $s = 4m_t^2$. Furthermore the external top quarks are on their mass shell. In addition we are only interested in hard corrections resulting from the real matching condition. Corrections to the cross section stemming from imaginary part of the matching coefficient, which takes into account the finite lifetime of the top quark, are discussed for SM in Ref. [22].

For the generation of the Feynman diagrams we use the `Mathematica` program `FeynArts` [23]. The amplitudes are further processed with the help of the programs `FormCalc` [24] and `FeynCalc` [25] which take the traces, map the occurring integrals to a standard basis and reduce the tensor integrals to a minimal set of scalar integrals usually denoted by A_0, B_0 and C_0. Since we have a quite particular momentum configuration it is not possible to use the above mentioned packages as black boxes but apply some modifications. In fact, the choice $s = 4m_t^2$ allows for a partial fractioning in the denominators of the loop integrands appearing in $t\bar{t}\gamma/Z$-vertex and box diagrams which effectively reduces the number of external legs by one. Consider, e.g., the integrand of a generic three-point function (omitting the $i\epsilon$ prescription)

$$\frac{1}{(p^2 + 2q_1 p - M_1^2 + m_t^2)(p^2 - 2q_2 p - M_2^2 + m_t^2)(p^2 - M_3^2)}, \tag{7}$$

where p is the integration momentum and $q_1^2 = q_2^2 = m_t^2$ are the squared momenta of the top quarks. After choosing $q_1 = q_2 = q/2$ and applying a partial fractioning one arrives at

$$\begin{aligned} &\frac{2}{\frac{M_1^2+M_2^2}{2} - M_3^2 - m_t^2}\left(\frac{1}{p^2 - \frac{M_1^2+M_2^2}{2} + m_t^2} - \frac{1}{p^2 - M_3^2}\right) \\ &\quad\times\left(\frac{1}{p^2 + q\cdot p - M_1^2 + m_t^2} + \frac{1}{p^2 - q\cdot p - M_2^2 + m_t^2}\right). \end{aligned} \tag{8}$$

As a consequence the result can be expressed in terms of only two-point functions. In a similar way one can express the box diagrams in terms of three-point functions.

III. SUPERSYMMETRIC QCD

In this section we consider the effects from supersymmetric QCD (SQCD) to the top-quark threshold production. There are only four contributing Feynman diagrams which are shown in Fig. 1. The one-loop QCD corrections are known since long [26] and the corresponding matching coefficient is defined via the relation

$$J_V^i = (1 + c_v^{(1)}) j_V^i = \left(1 - 2C_F \frac{\alpha_s}{\pi}\right) j_V^i. \tag{9}$$

This effect can be incorporated in the helicity amplitude by a simple rescaling of the tree-level contributions

$$h_{I,V}^{\rm QCD} = h_{I,V}^{\gamma,\rm tree} a_g^\gamma + h_{I,V}^{Z,\rm tree} a_g^Z. \tag{10}$$

Using the explicit expressions for $h_{I,V}^{\rm tree}$, one can already see that the contribution of a_X^Z to the relative correction Δ^X of the cross section is in general suppressed by factor 0.08 compared to the one resulting from contribution of a_X^γ. For the QCD the coefficients $a_g^{\gamma/Z}$ read

$$a_g^{\gamma/Z} = c_v^{(1)}. \tag{11}$$

Since we work in a supersymmetric framework we repeated the calculation of $c_v^{(1)}$ within dimensional reduction

[1] In this paper we use the THDM type II where u/d-type quarks couple to different Higgs doublets H_u/H_d. Note that the Higgs sector of the MSSM corresponds to the Higgs sector of THDM type II.

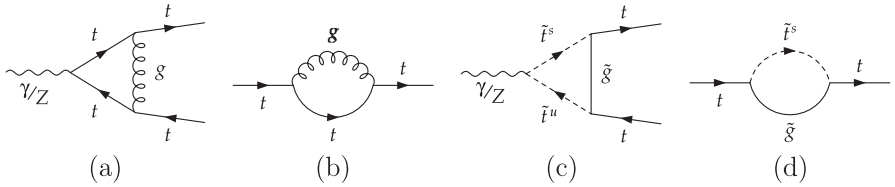

FIG. 1. QCD and SQCD diagrams. (a): Gluon contribution at the $t\bar{t}\gamma/Z$-vertex. (b): Gluon contribution to the top-quark self-energy. (c): Gluino contribution at the $t\bar{t}\gamma/Z$-vertex. (d): Gluino contribution to the top-quark self-energy.

[27]. Although both the one-loop vertex corrections and the result for the wave function counterterm are different from their counter parts in dimensional regularization we observe that the result given in Eq. (9) does not change. This is expected since at tree-level the strong coupling constant is absent.

The SQCD corrections can also be cast in the form of Eq. (10)

$$h_{I,V}^{\mathrm{SQCD}} = h_{I,V}^{\gamma,\mathrm{tree}} a_{\tilde{g}}^{\gamma} + h_{I,V}^{Z,\mathrm{tree}} a_{\tilde{g}}^{Z}, \tag{12}$$

with

$$\begin{aligned} a_{\tilde{g}}^{\gamma} &= \Gamma_{V,\tilde{g}}^{\gamma} + \delta Z_{V,\tilde{g}}^{t}, \\ a_{\tilde{g}}^{Z} &= \Gamma_{V,\tilde{g}}^{Z} + \delta Z_{V,\tilde{g}}^{t} - \frac{3}{8s_w^2 - 3}\delta Z_{A,\tilde{g}}^{t}, \end{aligned} \tag{13}$$

where $\Gamma_{V,\tilde{g}}^{\gamma/Z}$ represents the gluino contribution to the vector part of the one-loop vertex normalized by the corresponding tree-level coupling. The wave function renormalization constant $Z_{V/A,\tilde{g}}^{t} = 1 + \delta Z_{V/A,\tilde{g}}^{t}$ is defined in the on-shell scheme and renders the $\gamma t\bar{t}$ and $Zt\bar{t}$ vertex finite. The definition of both counter terms can be found in Appendix A, where they are expressed in terms of vector- (V) and axial-vector part (A) of the top-quark self-energy. The subscript $\tilde{g}$ reminds that only the diagrams involving a gluino are considered in each expression. Since the results are quite compact we present the analytical formulas for the individual contributions of the right-hand side of Eq. (13). The contributions to the wave function counterterm reads

$$\begin{aligned} \delta Z_{V,\tilde{g}}^{t} = \sum_{s=1}^{2} \frac{\alpha_s}{6\pi m_t^2} \{ & -2m_t^2[-2m_{\tilde{g}} m_t(\Omega_{s1s2} + \Omega_{s2s1}) + (m_t^2 + m_{\tilde{g}}^2 - m_{\tilde{t}_s}^2)(\Omega_{s1s1} + \Omega_{s2s2})]B_0'(m_t^2, m_{\tilde{g}}^2, m_{\tilde{t}_s}^2) + (\Omega_{s1s1} \\ & + \Omega_{s2s2})[A_0(m_{\tilde{t}_s}^2) - A_0(m_{\tilde{g}}^2)] + (m_{\tilde{g}}^2 - m_t^2 - m_{\tilde{t}_s}^2)(\Omega_{s1s1} + \Omega_{s2s2})B_0(m_t^2, m_{\tilde{g}}^2, m_{\tilde{t}_s}^2)\}, \\ \delta Z_{A,\tilde{g}}^{t} = \sum_{s=1}^{2} \frac{\alpha_s}{6\pi m_t^2} & (\Omega_{s1s1} - \Omega_{s2s2})\{A_0(m_{\tilde{g}}^2) - A_0(m_{\tilde{t}_s}^2) - (m_t^2 + m_{\tilde{g}}^2 - m_{\tilde{t}_s}^2)B_0(m_t^2, m_{\tilde{g}}^2, m_{\tilde{t}_s}^2)\}, \end{aligned} \tag{14}$$

and the vertex corrections are given by

$$\begin{aligned} \Gamma_{V,\tilde{g}}^{\gamma} = \sum_{s=1}^{2} & \frac{\alpha_s(\Omega_{s1s1} + \Omega_{s2s2})}{9\pi m_t^2(m_t^2 + m_{\tilde{g}}^2 - m_{\tilde{t}_s}^2)} \Big\{ 2m_t^2(m_t^2 - m_{\tilde{t}_s}^2)B_0(4m_t^2, m_{\tilde{t}_s}^2, m_{\tilde{t}_s}^2) + \frac{1}{2}(m_t^2 + m_{\tilde{g}}^2 - m_{\tilde{t}_s}^2)[A_0(m_{\tilde{g}}^2) - A_0(m_{\tilde{t}_s}^2) + 2m_t^2] \\ & - \frac{1}{2}[m_{\tilde{t}_s}^4 - 2(m_t^2 + m_{\tilde{g}}^2)m_{\tilde{t}_s}^2 + (m_{\tilde{g}}^2 - m_t^2)^2]B_0(m_t^2, m_{\tilde{g}}^2, m_{\tilde{t}_s}^2) \Big\}, \\ \Gamma_{V,\tilde{g}}^{Z} = \sum_{s,u=1}^{2} & \frac{\alpha_s[4s_w^2(\Omega_{s1u1} + \Omega_{s2u2}) - 3\Omega_{s1u1}](\Omega_{u1s1} + \Omega_{u2s2})}{9\pi m_t^2(m_{\tilde{t}_s}^2 + m_{\tilde{t}_u}^2 - 2m_{\tilde{g}}^2 - 2m_t^2)(8s_w^2 - 3)} \Big[\Big\{ +[m_{\tilde{t}_s}^4 - 2(m_t^2 + m_{\tilde{g}}^2)m_{\tilde{t}_s}^2 + (m_{\tilde{g}}^2 - m_t^2)^2]B_0(m_t^2, m_{\tilde{g}}^2, m_{\tilde{t}_s}^2) \\ & + [m_{\tilde{t}_s}^2 + m_{\tilde{t}_u}^2 - 2(m_t^2 + m_{\tilde{g}}^2)]\frac{1}{2}[A_0(m_{\tilde{g}}^2) - A_0(m_{\tilde{t}_s}^2) + 2m_t^2(1 + B_0(4m_t^2, m_{\tilde{t}_s}^2, m_{\tilde{t}_u}^2))] + [m_t^2(m_{\tilde{t}_s}^2 + m_{\tilde{t}_u}^2 + 2(m_{\tilde{g}}^2 - m_t^2)) \\ & - \frac{1}{4}(m_{\tilde{t}_s}^2 - m_{\tilde{t}_u}^2)^2]B_0(m_t^2, m_{\tilde{t}_s}^2, \frac{1}{2}m_{\tilde{t}_s}^2 + \frac{1}{2}m_{\tilde{t}_u}^2 - m_t^2) \Big\} + \{s \leftrightarrow u\} \Big]. \end{aligned} \tag{15}$$

In Eqs. (14) and (15) we introduced the abbreviations $\Omega_{ijkl} = U_{ij}U_{kl}^{\star}$ where U_{ij} are the elements of the top squark mixing matrix (cf. Appendix B). The conventions for the functions A_0 and B_0 are adapted from Refs. [24,28] where explicit results can be found. Further B_0' is the defined as derivative of B_0 with respect to the first argument. Our analytic formulas are in agreement with Ref. [29] where the result has been expressed in terms of a one-dimensional integral assuming a real mixing matrix for the top squarks.[2]

[2]The SQCD corrections for the hadronic Z boson decay and the quark pair production in electron positron annihilation have been considered in Refs. [30,31], respectively.

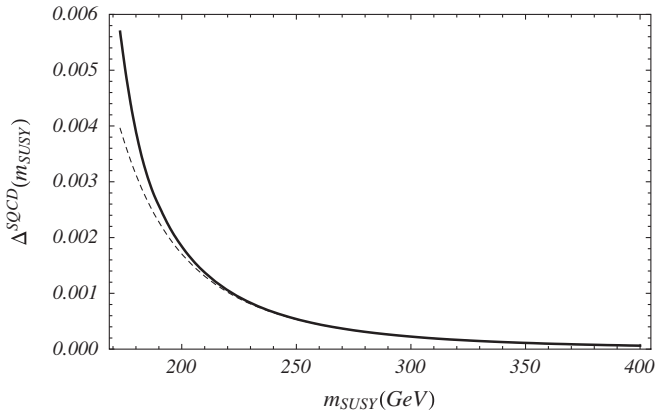

FIG. 2. $\Delta^{\mathrm{SQCD}} = 2a_{\tilde{g}}$ computed from Eq. (16) as a function of m_{SUSY}. The solid line represents the exact result and the dashed curve the expansion including terms up to order $(m_t^2/m_{\mathrm{SUSY}}^2)^5$.

It is instructive to consider the limit where all SUSY particles have a common mass m_{SUSY}. In this limit the above formulas are simplified significantly. In particular, the result becomes independent of the matrix elements U_{ij} and $\delta Z^t_{A,\tilde{g}} = 0$. We furthermore have $a_{\tilde{g}} = a^{\gamma}_{\tilde{g}} = a^{Z}_{\tilde{g}}$ which reads

$$\begin{aligned} a_{\tilde{g}}(m^2_{\mathrm{SUSY}}) &= \frac{4\alpha_s}{9m_t^2\pi}\left\{\frac{1}{2}m_t^2 - \frac{3}{2}m_t^4 B_0'(m_t^2, m^2_{\mathrm{SUSY}}, m^2_{\mathrm{SUSY}}) \right. \\ &\quad + (m^2_{\mathrm{SUSY}} - m_t^2)[B_0(m_t^2, m^2_{\mathrm{SUSY}}, m^2_{\mathrm{SUSY}}) \\ &\quad \left. - B_0(4m_t^2, m^2_{\mathrm{SUSY}}, m^2_{\mathrm{SUSY}})]\right\} \\ &= \frac{\alpha_s}{45\pi}\left\{y^2 + \frac{16}{21}y^3 + \frac{1}{2}y^4 + \frac{76}{231}y^5 + \mathcal{O}(y^6)\right\}. \end{aligned} \tag{16}$$

After the second equal sign we have expanded the result in terms of $y = m_t^2/m^2_{\mathrm{SUSY}}$.

Let us in the following discuss the numerical effects of the one-loop QCD and SQCD corrections. For $m_t = 173.1$ GeV and $\alpha_s^{(6)}(m_t) = 0.108$ the QCD corrections amount to $\Delta^{\mathrm{QCD}} = 18.3\%$ (corresponding to $\alpha_s^{(5)}(m_Z) = 0.1176$) and thus constitute the largest contribution.

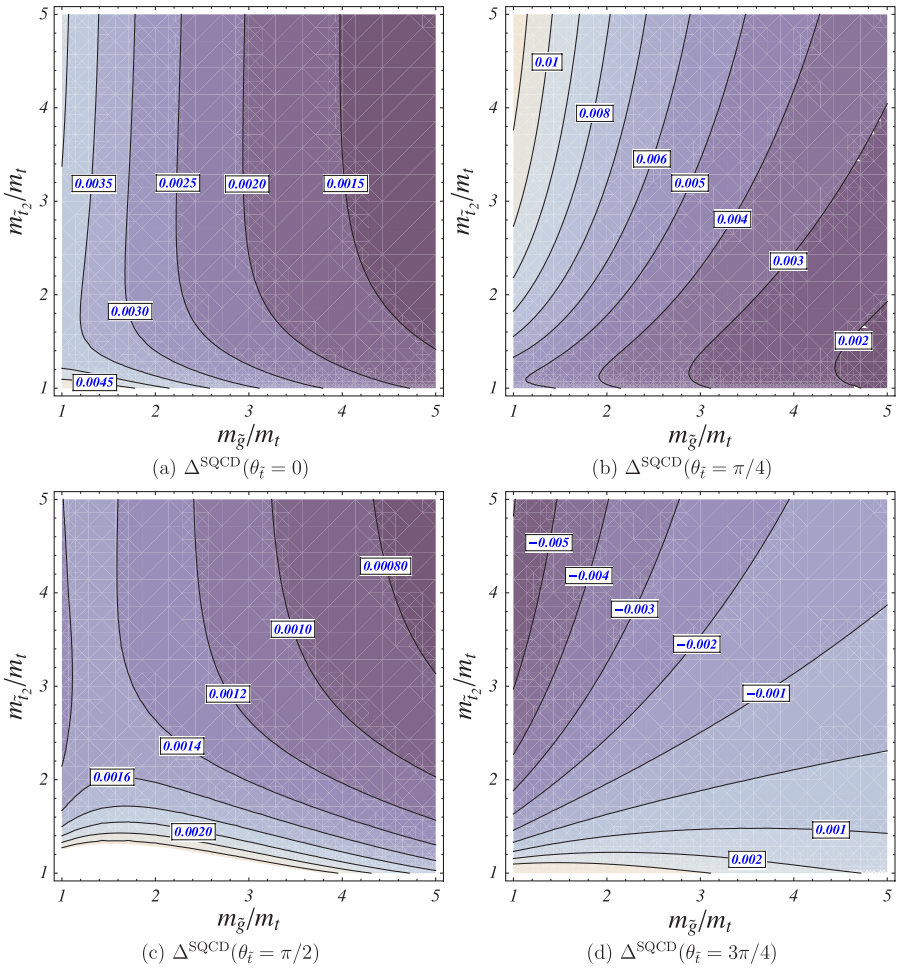

(a) $\Delta^{\mathrm{SQCD}}(\theta_{\tilde{t}} = 0)$ (b) $\Delta^{\mathrm{SQCD}}(\theta_{\tilde{t}} = \pi/4)$

(c) $\Delta^{\mathrm{SQCD}}(\theta_{\tilde{t}} = \pi/2)$ (d) $\Delta^{\mathrm{SQCD}}(\theta_{\tilde{t}} = 3\pi/4)$

FIG. 3 (color online). Δ^{SQCD} as a function of $m_{\tilde{t}_2}$ and $m_{\tilde{g}}$ (normalized to the top-quark mass) for $m_{\tilde{t}_1} = m_t$ and different values of the mixing angle $\theta_{\tilde{t}}$.

In the simplified scenario described by Eq. (16) one obtains the SQCD corrections as shown in Fig. 2. From the figure one can see that for $m_{\mathrm{SUSY}} > 200$ GeV the expansion agrees well with the exact result showing a relative deviation below 10%. For all $m_{\mathrm{SUSY}} > m_t$ the relative correction to the threshold cross section stays below 0.6%. The size of the SQCD corrections in a non-universal SUSY mass scenario is shown in Fig. 3 where Δ^{SQCD} is plotted as a function of $m_{\tilde{t}_2}$ and $m_{\tilde{g}}$ for $m_{\tilde{t}_1} = m_t$. Since our results are π-periodic in $\theta_{\tilde{t}}$ we have chosen for illustration the four values $\theta_{\tilde{t}} \in \{0, \frac{\pi}{4}, \frac{\pi}{2}, \frac{3\pi}{4}\}$. The figures show, that only for light masses of the second top squark ($m_{\tilde{t}_2} \lesssim 2m_t$) Δ^{SQCD} can have a strong dependence on $m_{\tilde{t}_2}$.

In general one observes corrections below 1% which become negligible for large masses of the SUSY particles. A correction factor above 1% is only observed for $\theta_{\tilde{t}} = \pi/4$ and relatively light gluino masses of the order of the top-quark mass which are excluded within the MSSM [32].

IV. ELECTROWEAK CORRECTIONS IN THE THDM AND THE MSSM

QCD corrections only affect the $\gamma t\bar{t}/Zt\bar{t}$ vertex. On the other hand, electroweak corrections require also the inclusion of the $e^+e^-\gamma/e^+e^-Z$ vertex and furthermore of gauge boson self-energy and box contributions which are necessary in order to arrive at a finite and gauge parameter independent result. Typical Feynman diagrams contributing to the individual building blocks are shown in Fig. 4 for the SM and in Fig. 5 for the MSSM. Because of the

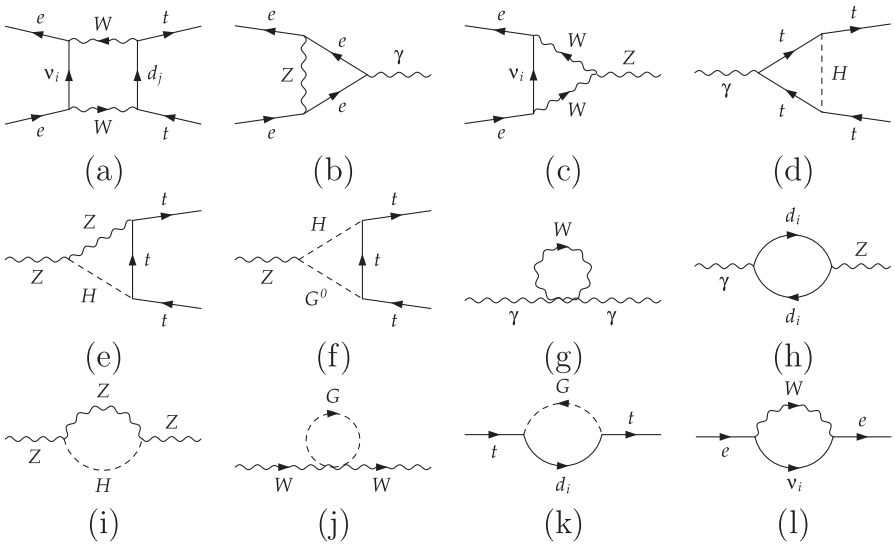

FIG. 4. Typical Feynman diagrams contributing to Δ^{SM}.

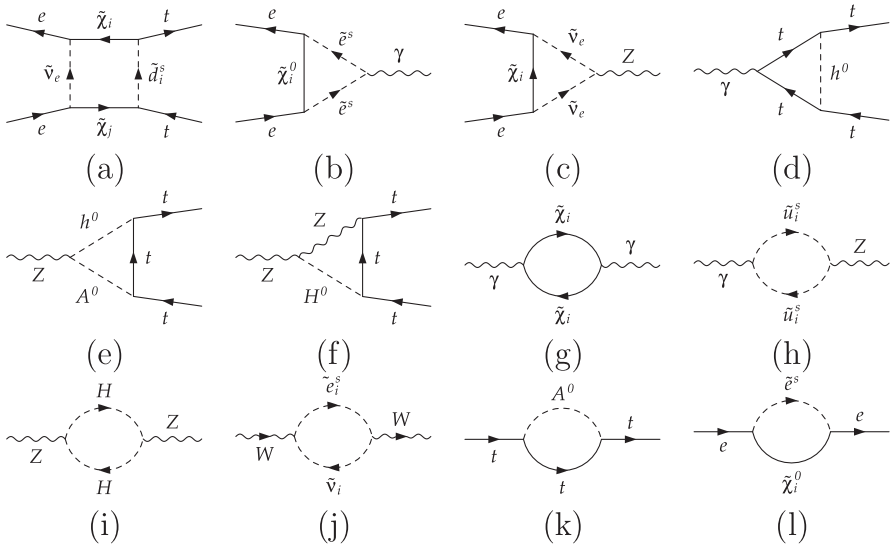

FIG. 5. Typical Feynman diagrams contributing to Δ^{MSSM}.

renormalization procedure (we follow Refs. [33,34]) also W boson and fermion self-energy contributions have to be computed which are also shown in Figs. 4 and 5. They are used in order to render the four building blocks individually finite which is quite convenient to deal with.

In a first step we have used our setup in order to compute the SM contribution. We find complete agreement with Refs. [18,19,21]. Afterwards the THDM model has been considered and the results from Ref. [20] have been reproduced.[3] Let us note that for vanishing bottom quark mass the corrections in the THDM model can easily be obtained from the analytical results for Higgs- and Goldstone boson contribution calculated in the SM by adjusting the coupling factors and boson masses in the loop diagrams.

Results for the MSSM are not yet available in the literature. However, it is possible to compare our results for the vector boson self-energies with Ref. [35] where the top-quark production has been considered above the threshold. As far as the box contribution is concerned, new kind of diagrams occur in the MSSM where the electron and positron in the initial state are not part of the same fermion line (and similarly for the top quarks in the final state), cf. Fig. 5(a). Because of the different tensor structure, originating from the Majorana character of charginos and neutralinos, it is not straightforward to process these contributions with our setup. On the other hand, it is possible to extract the relative correction to the cross section at the threshold by taking the limit $s \to 4m_t^2$ since these diagrams only involve heavy particles inside the loop. However, due to the numerical properties of the loop functions [24] the limit can not be taken naively. Instead we evaluate the result of Ref. [35] for the box contribution above threshold and extrapolate to $s = 4m_t^2$. In this way we obtain the threshold contribution for the new box diagrams with three significant digits which is sufficient for the phenomenological analysis. We have applied the same procedure for the SM box contributions which provides both a cross check on our analytical calculation and the very procedure for extracting the threshold contribution.

Because of the occurrence of many different masses and mixing angles the remaining general expression is quite lengthy in the case of the MSSM. Thus, in the following we will only discuss the numerical effects. In Ref. [36] a package is provided which allows the numerical evaluation of the corrections described in this paper. It uses `Mathematica` as front-end and calls Fortran for the time-consuming parts of the calculation. In addition an interface to SPheno [37] is provided, which generates numerical values for the masses and mixing angles on the basis of a certain SUSY breaking scenario.

[3]In Ref. [20] the expression for $a^Z_{Zh^0}$ is proportional to $\cos(\beta - \alpha)$ which should be replaced by $\sin(\beta - \alpha)$.

TABLE I. Input values for the SPS scenarios as defined in Refs. [38,39]. All masses are given in GeV and $\mathrm{sgn}(\mu) = 1$.

	Points				Slopes	
Label	m_0	$m_{1/2}$	A_0	$\tan\beta$	m_0	A_0
SPS1a'	70	250	−300	10	-	-
SPS1a	100	250	−100	10	$0, 4m_{1/2}$	$-0, 4m_{1/2}$
SPS1b	200	400	0	30	-	-
SPS2	1450	300	0	10	$2m_{1/2} + 850$	0
SPS3	90	400	0	10	$0, 25m_{1/2} - 10$	0
SPS4	400	300	0	50	-	-
SPS5	150	300	−1000	5	-	-

In the numerical discussion we will restrict ourselves to the SUSY breaking scenario based on minimal supergravity (mSUGRA) and use the snowmass points and slopes (SPS) [38,39] in order get an impression of size of the corrections. In addition to the five mSUGRA parameters m_0, $m_{1/2}$, $\tan\beta$, A_0 and $\mathrm{sgn}(\mu)$ (cf. Table I) which serve as input for the spectrum generator we use the following input values for the remaining SM parameters [40–42][4]

$$\begin{aligned} m_W &= 80.40\ \text{GeV}, \qquad m_Z = 91.1876\ \text{GeV}, \\ c_w^2 &= m_W^2/m_Z^2, \qquad m_t = 173.1\ \text{GeV}, \\ m_b &= 4.2\ \text{GeV}, \qquad \alpha^{-1} = 137.036, \\ \Delta\alpha^{(5)}_{\text{had}}(m_Z) &= 277.45 \times 10^{-4}, \\ \Delta\alpha_{\text{lep}}(m_Z) &= 314.97 \times 10^{-4}. \end{aligned} \tag{17}$$

In a first step our `Mathematica` program transfers the input values to the spectrum generator `SPheno` [37] which produces numerical values for all unknown MSSM parameters relevant for our analysis. The output is automatically imported into `Mathematica` and afterwards used in order to evaluate the THDM or MSSM corrections. More details about the functionality of our package is provided via the usual `Mathematica` internal documentation and example files which in addition automatically generate the plots and tables shown in this paper.

The numerical impact of the corrections in different mSUGRA scenarios can be seen in Table II where $\Delta^{\text{SM EW}}$, $\Delta^{\text{THDM EW}}$ and $\Delta^{\text{MSSM EW}}$ are evaluated for several SPS points.[5] Note that $\Delta^{\text{SM EW}}$ varies since the SM Higgs boson is identified with the lightest MSSM Higgs boson.

The SM corrections amount to a sizeable shift of about 15% which get reduced by roughly 5% to 6% in the case of the THDM. The main reason for this reduction is the smaller coupling of the top quark to the light Higgs boson. At the same time only numerically small contributions

[4]Following Ref. [43] we replace light fermion contributions to the derivative of the photon vacuum polarization function by $\Delta\alpha^{(5)}_{\text{had}}(m_Z)$ and $\Delta\alpha_{\text{lep}}(m_Z)$.

[5]We add EW to the superscript in order to make clear that only electroweak and no strong corrections are considered.

TABLE II. Numerical values for $\Delta^{X\,\mathrm{EW}}$ $X \in$ {SM, THDM, MSSM} for various SPS scenarios.

	SPS1a	SPS1a'	SPS1b	SPS2	SPS3	SPS4	SPS5
$\Delta^{\mathrm{SM\,EW}}$	0.152	0.151	0.149	0.149	0.149	0.150	0.149
$\Delta^{\mathrm{THDM\,EW}}$	0.097	0.096	0.093	0.091	0.093	0.099	0.094
$\Delta^{\mathrm{MSSM\,EW}}$	0.096	0.096	0.093	0.089	0.093	0.101	0.094

arise from the diagrams involving heavy Higgs bosons. In Table II one observes only a marginal difference between the THDM and the MSSM. It is thus instructive to have a closer look at the dependence on $m_{1/2}$ as suggested by the SPS scenarios. For illustration we show in Fig. 6 the comparison of $\Delta^{\mathrm{SM\,EW}}$, $\Delta^{\mathrm{THDM\,EW}}$ and $\Delta^{\mathrm{MSSM\,EW}}$ for SPS1 and SPS2. In both cases we observe only small corrections beyond the THDM, i.e. from the neutralino and chargino sector of the MSSM. Larger deviations of the order of 0.5% are only observed for those values of $m_{1/2}$ where the corresponding chargino masses are close to the top-quark mass. This becomes clear in Fig. 7 where we show the correction of the finite building blocks separately for the case of SPS1a. One can see a relatively strong variation in the dashed curve which shows the contributions from the charginos. It is interesting to note that the peak around $m_{1/2} \approx 150$ GeV in Δ_{Box} is clearly visible in Fig. 6(a) whereas a cancelation among the various parts occurs for the peak close to $m_{1/2} \approx 250$ GeV. For comparison we plot in Fig. 7(d) the contribution from SQCD (dashed-dotted). For $m_{1/2} \gtrsim 150$ GeV it is smaller than the chargino contribution. Corrections above 0.5% are only reached for relatively small values of $m_{1/2}$ which corresponds to small values of the gluino mass. Let us finally mention that we performed our calculation in the THDM and MSSM for finite bottom quark mass and investigated possible large corrections for higher values of $\tan\beta$. However, even for the mSUGRA scenario SPS4 where $\tan\beta = 50$, the result for massless bottom quark is $\Delta^{\mathrm{MSSM\,EW}}_{m_b=0} = 0.099$, thus the effect of finite bottom quark mass adds 0.002 to $\Delta^{\mathrm{MSSM\,EW}}_{m_b=0}$ (see Table II).

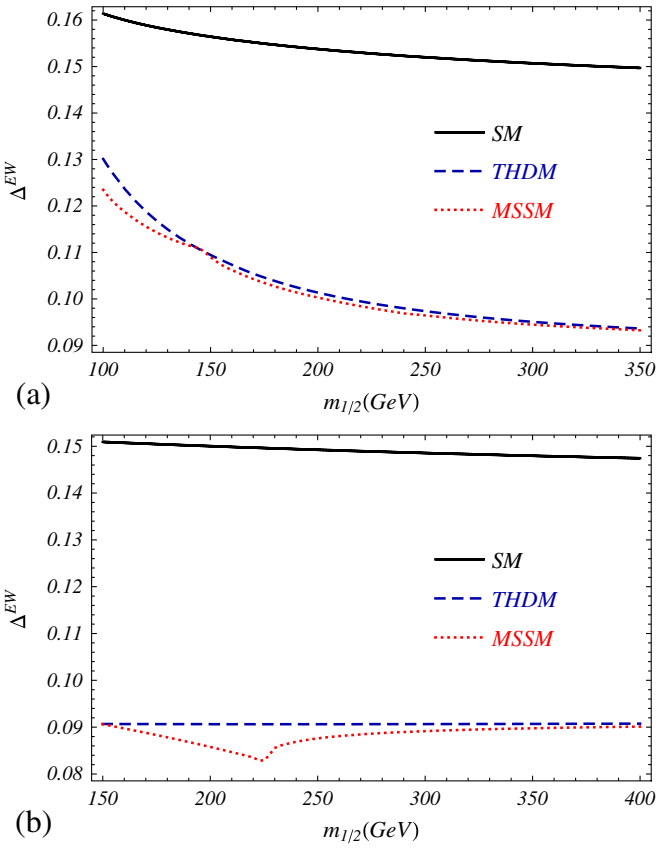

FIG. 6 (color online). $\Delta^{X\,\mathrm{EW}}$ for $X \in$ {SM, THDM, MSSM} as function of the unified mSUGRA gaugino mass $m_{1/2}$ for (a) SPS1a and (b) SPS2.

V. CONCLUSIONS

In this paper we investigated the complete weak and strong one-loop corrections within the MSSM to the threshold production of top-quark pairs at a future e^+e^- linear collider. For the SM, THDM, QCD and SQCD corrections we confirmed the results in the literature, the genuine supersymmetric electroweak corrections are new.

As far as the numerical importance is concerned, the electroweak SM corrections amount up to +15% for light Higgs masses. After extending the Higgs sector we observe for the SPS scenarios a screening of about −5% to −6% in the THDM (type II). The pure supersymmetric corrections from the chargino, neutralino and the strong sector are below 1% in most of the parameter space.

ACKNOWLEDGMENTS

We would like to thank Christian Schappacher for sharing his program and knowledge about `FormCalc`, Thomas Hahn for his support, and J. H. Kühn for valuable discussions. This work was supported by the DFG through the SFB/TR 9 "Computational Particle Physics" and by the BMBF through Grant No. 05H09VKE.

APPENDIX A: ON-SHELL COUNTERTERMS

In this appendix we discuss the definition of the counterterms appearing in Eq. (13). In order to define the fermionic on-shell counterterms one needs the coefficient functions of the tensor decomposition from the corresponding fermion self-energy:

$$\Sigma(q, m) = m\Sigma_s(q^2, m) + \not{q}\Sigma_v(q^2, m) + \not{q}\gamma^5\Sigma_a(q^2, m). \tag{A1}$$

They can be extracted with the help of the following projections:

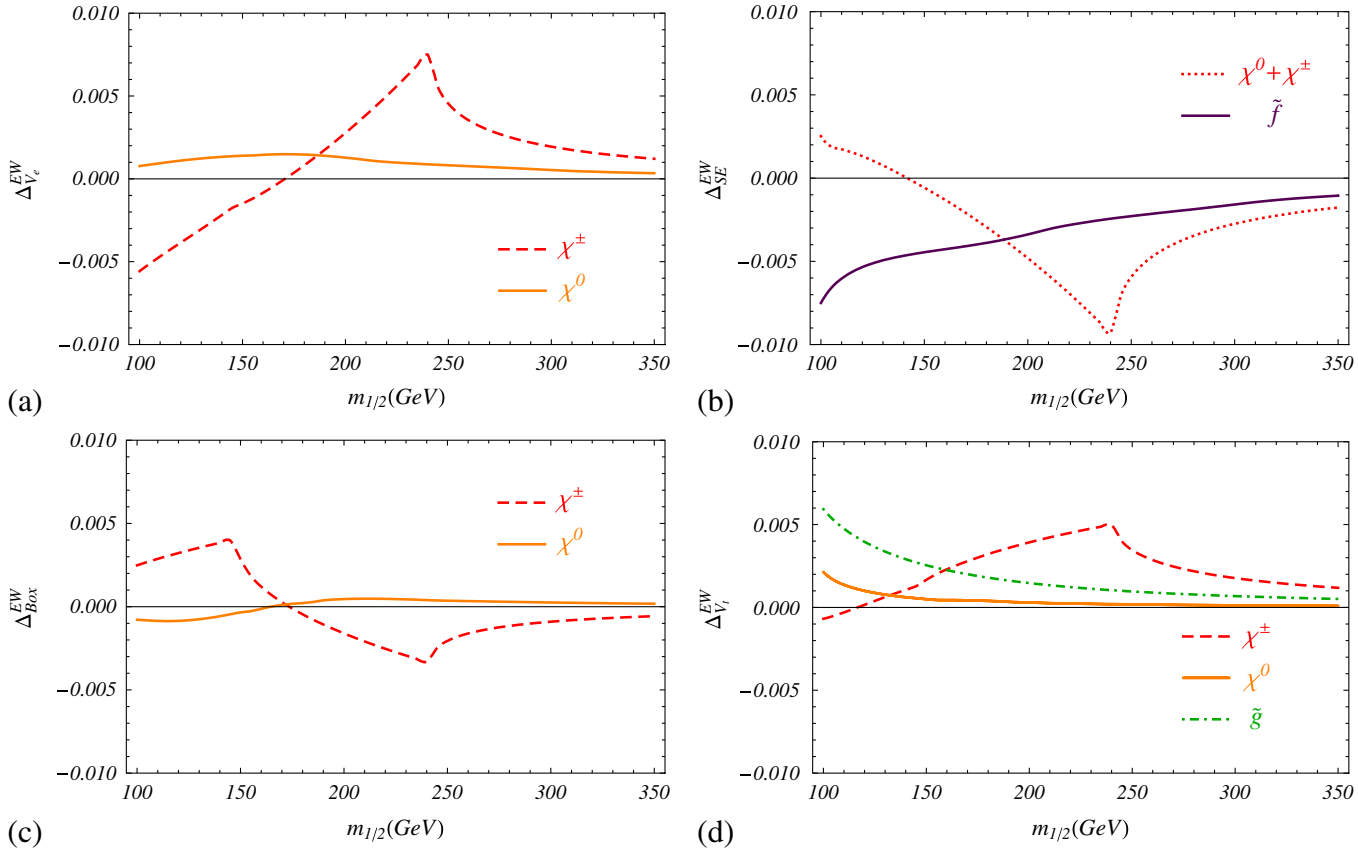

FIG. 7 (color online). Contributions of the building blocks to $\Delta^{\mathrm{MSSM\,EW}}$ in the MSSM as function of the unified gaugino mass $m_{1/2}$ for SPS1a: (a) electron vertex, (b) vector boson self-energies, (c) box and (d) top-quark vertex. In (d) the SQCD corrections are shown for comparison.

$$\Sigma_s(q^2, m) = \frac{1}{4m}\,\mathrm{tr}\{\Sigma(q, m)\}, \tag{A2a}$$

$$\Sigma_v(q^2, m) = \frac{1}{4q^2}\,\mathrm{tr}\{\not{q}\Sigma(q, m)\}, \tag{A2b}$$

$$\Sigma_a(q^2, m) = \frac{1}{4q^2}\,\mathrm{tr}\{\gamma^5\not{q}\Sigma(q, m)\}. \tag{A2c}$$

The wave function counterterms are then given by

$$\delta Z_V^f = -\Sigma_v(m_f^2, m_f) - 2m_f^2\frac{\partial}{\partial q^2}[\Sigma_v(q^2, m_f) + \Sigma_s(q^2, m_f)]|_{q^2=m_f^2}, \tag{A3}$$

$$\delta Z_A^f = \Sigma_a(m_f^2, m_f). \tag{A4}$$

APPENDIX B: MIXING MATRICES

Let us for definiteness provide in this Appendix the definition of the mixing matrix $\mathbf{U}_{\tilde{f}} = (U_{ij})$ used in Eqs. (14) and (15). We work with flavor diagonal sfermion mixings, where the left and right-handed sfermion fields $\tilde{f}_L$ and $\tilde{f}_R$ are connected to the mass eigenstates $\tilde{f}_1$ and $\tilde{f}_2$ via

$$\begin{pmatrix}\tilde{f}_1\\ \tilde{f}_2\end{pmatrix} = \mathbf{U}_{\tilde{f}}\begin{pmatrix}\tilde{f}_L\\ \tilde{f}_R\end{pmatrix}. \tag{B1}$$

The 2×2 mixing matrix $\mathbf{U}_{\tilde{f}}$ diagonalizes the mass matrix of the corresponding sfermion $\tilde{f}$:

$$\mathbf{U}_{\tilde{f}}\mathbf{m}^2_{\tilde{f}}\mathbf{U}^{\dagger}_{\tilde{f}} = \begin{pmatrix}m^2_{\tilde{f}_1} & 0\\ 0 & m^2_{\tilde{f}_2}\end{pmatrix}. \tag{B2}$$

In the case where the mass matrix $\mathbf{m}^2_{\tilde{f}}$ contains only real entries, one can choose $\mathbf{U}_{\tilde{f}}$ to be orthogonal. For its parametrization only one angle $\theta_{\tilde{f}}$ is needed and the transformation from mass to gauge eigenstates can be written as follows:

$$\begin{aligned}\tilde{f}_1 &= \tilde{f}_L\cos\theta_{\tilde{f}} + \tilde{f}_R\sin\theta_{\tilde{f}},\\ \tilde{f}_2 &= \tilde{f}_R\cos\theta_{\tilde{f}} - \tilde{f}_R\sin\theta_{\tilde{f}}.\end{aligned} \tag{B3}$$

[1] A. H. Hoang *et al.*, Eur. Phys. J. direct C **2**, 1 (2000).
[2] B. A. Kniehl, A. A. Penin, V. A. Smirnov, and M. Steinhauser, Nucl. Phys. **B635**, 357 (2002).
[3] A. A. Penin, V. A. Smirnov, and M. Steinhauser, Nucl. Phys. **B716**, 303 (2005).
[4] M. Beneke, Y. Kiyo, and K. Schuller, Nucl. Phys. **B714**, 67 (2005).
[5] P. Marquard, J. H. Piclum, D. Seidel, and M. Steinhauser, Nucl. Phys. **B758**, 144 (2006).
[6] D. Eiras and M. Steinhauser, Nucl. Phys. **B757**, 197 (2006).
[7] M. Beneke, Y. Kiyo, and K. Schuller, Phys. Lett. B **658**, 222 (2008).
[8] M. Beneke, Y. Kiyo, and A. A. Penin, Phys. Lett. B **653**, 53 (2007).
[9] M. Beneke and Y. Kiyo, Phys. Lett. B **668**, 143 (2008).
[10] Y. Kiyo, D. Seidel, and M. Steinhauser, J. High Energy Phys. 01 (2009), 038.
[11] P. Marquard, J. H. Piclum, D. Seidel, and M. Steinhauser, Phys. Lett. B **678**, 269 (2009).
[12] A. V. Smirnov, V. A. Smirnov, and M. Steinhauser, Phys. Lett. B **668**, 293 (2008).
[13] M. Beneke, Y. Kiyo, and K. Schuller, Proc. Sci., RADCOR2007 (2007) 051.
[14] A. H. Hoang, A. V. Manohar, I. W. Stewart, and T. Teubner, Phys. Rev. Lett. **86**, 1951 (2001).
[15] A. H. Hoang, A. V. Manohar, I. W. Stewart, and T. Teubner, Phys. Rev. D **65**, 014014 (2001).
[16] A. Pineda and A. Signer, Nucl. Phys. **B762**, 67 (2007).
[17] M. Martinez and R. Miquel, Eur. Phys. J. C **27**, 49 (2003).
[18] B. Grzadkowski, J. H. Kühn, P. Krawczyk, and R. G. Stuart, Nucl. Phys. **B281**, 18 (1987).
[19] R. J. Guth and J. H. Kühn, Nucl. Phys. **B368**, 38 (1992).
[20] A. Denner, R. J. Guth, and J. H. Kühn, Nucl. Phys. **B377**, 3 (1992).
[21] A. H. Hoang and C. J. Reisser, Phys. Rev. D **74**, 034002 (2006).
[22] A. H. Hoang and C. J. Reisser, Phys. Rev. D **71**, 074022 (2005).
[23] T. Hahn, Comput. Phys. Commun. **140**, 418 (2001).
[24] T. Hahn and M. Perez-Victoria, Comput. Phys. Commun. **118**, 153 (1999).
[25] R. Mertig, M. Böhm, and A. Denner, Comput. Phys. Commun. **64**, 345 (1991).
[26] G. Källen and A. Sabry, K. Dan. Vidensk. Selsk. Mat. Fys. Medd. **29**, 1 (1955).
[27] W. Siegel, Phys. Lett. B **84**, 193 (1979).
[28] G. Passarino and M. J. G. Veltman, Nucl. Phys. **B160**, 151 (1979).
[29] S. f. Su and M. B. Wise, Phys. Lett. B **510**, 205 (2001).
[30] K. Hagiwara and H. Murayama, Phys. Lett. B **246**, 533 (1990).
[31] A. Djouadi, M. Drees, and H. Konig, Phys. Rev. D **48**, 3081 (1993).
[32] C. Amsler *et al.* (Particle Data Group), Phys. Lett. B **667**, 1 (2008).
[33] M. Böhm, H. Spiesberger, and W. Hollik, Fortschr. Phys. **34**, 687 (1986).
[34] W. Hollik, Report No. MPI-PH-93-21, Report No. BI-TP-93-16, 1993.
[35] W. Hollik and C. Schappacher, Nucl. Phys. **B545**, 98 (1999).
[36] http://www-ttp.particle.uni-karlsruhe.de/Progdata/ttp09/ttp09-20/.
[37] W. Porod, Comput. Phys. Commun. **153**, 275 (2003).
[38] B. C. Allanach *et al.*, in *Proc. of the APS/DPF/DPB Summer Study on the Future of Particle Physics (Snowmass 2001)*, edited by N. Graf [Eur. Phys. J. C].
[39] J. A. Aguilar-Saavedra *et al.*, Eur. Phys. J. C **46**, 43 (2006).
[40] Tevatron Electroweak Working Group, CDF Collaboration, and D0 Collaboration, arXiv:0903.2503.
[41] D. Abbaneo *et al.* (LEP Electroweak Working Group), http://lepewwg.web.cern.ch/LEPEWWG/.
[42] J. H. Kühn and M. Steinhauser, Phys. Lett. B **437**, 425 (1998).
[43] A. Denner, Fortschr. Phys. **41**, 307 (1993).